SANDIA REPORT

SAND97–2319 • UC–404
Unlimited Release
Printed September 1997

Atomic-Scale Measurement of Liquid Metal Wetting and Flow

N. D. Shinn, C. Daly, R. Limary, T. M. Mayer, T. A. Michalske, T. Kim,
R. M. Crooks, U. Landman

Prepared by
Sandia National Laboratories
Albuquerque, New Mexico 87185 and Livermore, California 94550

Sandia is a multiprogram laboratory operated by Sandia Corporation,
a Lockheed Martin Company, for the United States Department of
Energy under Contract DE-AC04-94AL85000.

Sandia National Laboratories

Issued by Sandia National Laboratories, operated for the United States Department of Energy by Sandia Corporation.

Available to DOE and DOE contractors from
Office of Scientific and Technical Information
PO Box 62
Oak Ridge, TN 37831

Prices available from (615) 576-8401, FTS 626-8401

Available to the public from
National Technical Information Service
US Department of Commerce
5285 Port Royal Rd
Springfield, VA 22161

NTIS price codes
Printed copy: A08
Microfiche copy: A01

Category UC-404

SAND 97-2319
Unlimited Release
Printed September 1997

Atomic-Scale Measurement of Liquid Metal Wetting and Flow

N. D. Shinn, C. Daly[†], R. Limary[#], T. M. Mayer, T. A. Michalske
Surface & Interface Science Department
Sandia National Laboratories
P. O. Box 5800
Albuquerque, NM 87185-1413

T. Kim
Department of Chemistry
Hallym University
Kang-Won Do, 200-702, South Korea

R. M. Crooks
Department of Chemistry
Texas A&M University
College Station, TX 77843-3255

U. Landman
School of Physics
Georgia Institute of Technology
Atlanta, GA 30332-0430

Abstract

The flow behavior of liquid metals at solid interfaces is critically important to successful welding, brazing, soldering and the synthesis of metal/ceramic composites. Continuum flow models frequently fail to reliably predict wetting behavior because they are based upon bulk fluid properties, rather than microscopic flow processes at the actual solid/liquid interface. Improved understanding of interfacial liquid flow is hindered by the paucity of experimental measurements at this microscopic level. This report describes a new approach, Acoustic Wave Damping (AWD), to measuring viscoelastic properties of liquid metal layers in the nanometer thickness regime. The AWD experiment measures the frequency response of a quartz crystal microbalance in contact with an viscoelastic layer. An equivalent circuit model and continuum acoustic theory relate this electrical response to mechanical energy storage and dissipative loss. For viscoelastic layers of known thickness and density, a quantitative complex shear modulus can be determined from the AWD data. Studies of self-assembled monolayers (SAMs) demonstrate sensitivity to monolayer structure and bonding. Molecular dynamics simulations relate these atomistic properties to the ensemble response. AWD measurements of ultra-thin liquid indium layers reveal metastable undercooling for 10-50nm thick indium layers. Continued refinement of the AWD technique and the addition of complementary interface characterization techniques will enable definitive studies of ultra-thin molten metals.

† Present Address: U.S. Naval Research Laboratory, Code 6670, Washington, DC, 20375.
# Present Address: Department of Chemical Engineering, The University of Texas at Austin, Austin, TX, 78712.

Contents

1.0 Introduction

From advanced engineered materials to the commonplace solder joint, the flow properties of thin liquid metal layers play an important role in the synthesis, processing and stability of materials and structures. For example, the fabrication of light-weight metal-matrix structural composites involves infusing the microscopic channels of a porous ceramic precursor with a molten metal [1]. Similarly, in joining technologies such as soldering, brazing and welding, the wetting of the interface between two solids by a liquid metal is a prerequisite to strong interfacial bonding. Incomplete interfacial wetting during materials synthesis or joining is a pervasive problem that can lead to unpredictable and catastrophic structural failure with costly consequences.

Solutions to these problems require an increased understanding of wetting [2]. Modern theories for liquid spreading combine a thermodynamic driving force with a viscous dissipation term that is derived from continuum hydrodynamics models for fluid flow. In these models, a steady state spreading velocity is determined by setting a balance between the driving force for wetting and the energy loss due to viscous dissipation in the spreading droplet [3]. Unfortunately, these macroscopic models have a serious limitation. When they are extended to the microscopic dimensions of the spreading front, the forces that are predicted in the liquid diverge and the viscous dissipation term becomes unbounded. In a physical sense, the failure of the current models for liquid spreading is a direct result of applying macroscopic concepts for fluid flow to the microscopic length scales at which wetting takes place.

The spreading of *any* macroscopic liquid requires that particles (atoms or molecules) at the leading edge of the droplet preferentially adsorb onto the bare substrate rather than remain within the fluid environment. This realization necessitates developing models based upon accurate atomic-scale physics, and validating these models by microscopic flow measurements. This report describes a new experimental approach, called Acoustic Wave Damping (AWD), to measuring the viscosity, or more generally the viscoelasticity, of ultra-thin layers. We have three objectives: (1) to develop the AWD method for quantitative measurements of the mechanical properties of nanometer thick layers; (2) to use AWD measurements to relate continuum theory and atomic-level simulations of mechanics; and (3) to develop high-temperature AWD technology for studies of ultra-thin liquid metal layers. Section 2 summarizes the AWD experiment, data analysis, and theory. The applicability of the AWD method to ultra-thin layers is first demonstrated by viscoelastic measurements of self-assembled monolayers in Section 3. Molecular dynamics simulations are also reported which provide an atomistic viewpoint into the ensemble response. Lastly, we report the first application of AWD to ultra-thin liquid metal layers, where pre-melting transient damping and metastable undercooling phenomena have been observed.

2.0 The Acoustic Wave Damping Technique

Acoustic Wave Damping exploits the piezoelectric properties of certain materials to detect mechanical changes at the interface between the material and its environment [4]. For example, the addition of a fractional atomic monolayer onto the surface of a Quartz Crystal Microbalance (QCM) can be detected accurately by a shift in the QCM resonant frequency [5]. The QCM, shown in figure 1, is perhaps the most common example of a transverse shear mode resonator, which in general consists of thin metal electrodes patterned on the parallel faces of a single crystal wafer oriented along a specific piezoelectric axis. The crystallographic axis is chosen such that only one vibrational mode is activated when a voltage is applied across the parallel electrodes. In the linear response regime, the displacements of a transverse shear mode resonator occur only in planes parallel to the electrode surfaces and are proportional to the applied voltage across the electrodes.

When an ac voltage of frequency ν is applied to the QCM, resonance occurs if the corresponding wavelength, λ, satisfies the relation $N \bullet (\lambda/2) = d$, where N is an odd integer, d is the thickness of the quartz wafer, and $\nu \bullet \lambda = v$, the velocity of sound in quartz. This corresponds to a sinusoidal displacement profile through the quartz wafer with maxima occurring in opposite directions at the upper and lower electrodes, respectively, and zero displacement in a plane half-way between the electrode surfaces. Even multiples of $(\lambda/2)$ are prohibited by symmetry. Thus, when operating at resonance or its overtones, the parallel QCM electrodes are undergoing sinusoidal lateral accelerations of equal magnitude but in opposite directions.

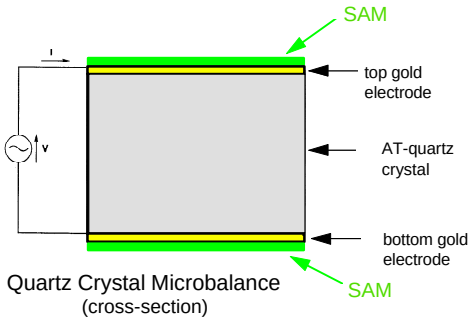

Fig. 1: Schematic cross-section of a quartz crystal microbalance (QCM) with oscillator circuit.

The resonant frequency of a QCM is determined by its thickness and operating environment. In figure 2, we show typical response data for a commercial, nominal 5 MHz QCM operating in a vacuum environment. A network analyzer is used to measure the electrical admittance as a function of excitation frequency near the fundamental resonance and at each successive overtone. The solid and open circles represent the real and imaginary components of the complex admittance (the reciprocal of impedance). For N=1, the frequency at which the admittance is maximized is denoted as the series resonance and also corresponds to a purely real impedance. In most applications, the QCM is driven by an oscillator circuit designed to operate at the series resonance frequency.

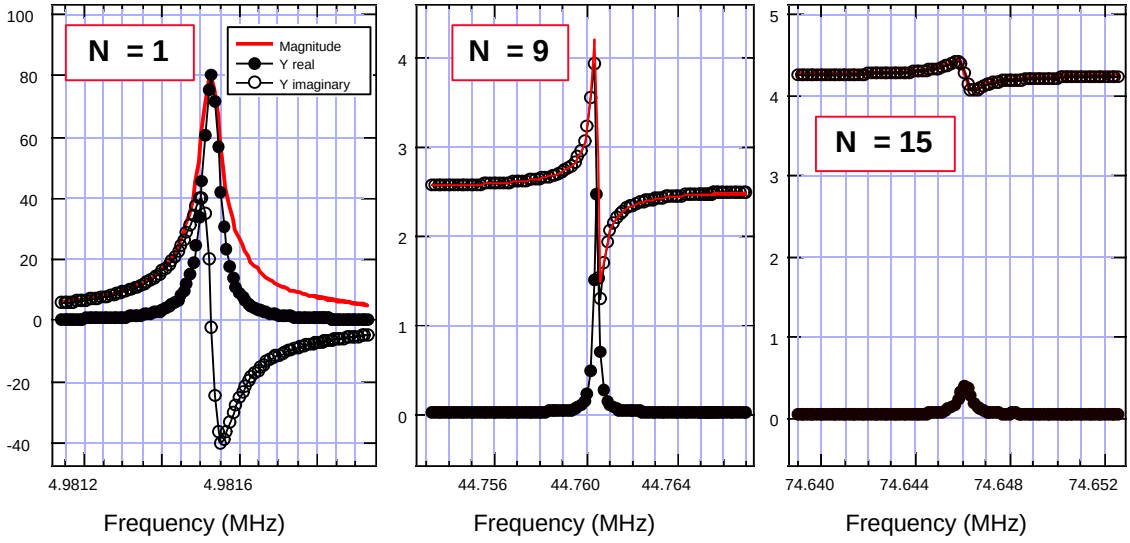

Fig. 2: Measured admittance as a function of frequency near the fundamental (N=1) and representative overtone frequencies of a quartz crystal microbalance resonator.

However, the resonator may also be driven at its overtone frequencies to produce higher lateral accelerations at the electrode surfaces. The practical limit to operation at higher overtones is the sensitivity of the network analyzer. If a QCM is operating in an environment other than vacuum, then the moving electrode surfaces will mechanically couple to the surrounding medium. For example, impinging gas molecules will exchange

momentum with the moving electrode surfaces and adsorption upon the electrode surface will add an inertial load to the QCM. These interfacial effects alter the electrical response of the QCM in predictable ways, namely changes in the resonant frequency and/or admittance amplitude [4,6]. In brief, if the QCM electrodes are in contact with an elastic solid or viscous fluid, the QCM response is determined by the elastic modulus or viscosity, respectively, of the layer. This is the basic idea that is exploited in the present work on ultra-thin films.

For frequencies near resonance, the equivalent circuit model shown in figure 3 is a conceptually simple representation of the QCM [4,6]. In this model, C_o is the static capacitance of the QCM and associated mounting connections. The dynamic element C_1 represents the mechanical elasticity of the vibrating QCM, the dynamic inductance L_1 is a measure of the vibrating mass, and the equivalent resistance R_1 corresponds to the total loss of mechanical energy due to internal friction and energy dissipated to the surrounding medium and supporting structures. If the QCM electrodes are in contact with a viscoelastic film, then additional circuit elements are used to represent energy storage, L_2, and dissipation, R_2, within the film.

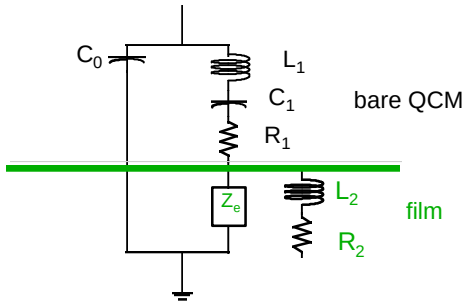

Fig. 3: Equivalent circuit model for the impedance of a quartz crystal microbalance (QCM) resonator with and without an ultra-thin viscoelastic film on the electrode surfaces.

For a clean QCM operating in vacuum, the three parameters C_1, L_1 and R_1 completely determine the complex impedance at any frequency near the series resonance. Hence, by measuring the impedance (or admittance) at three frequencies near resonance, a unique parameter set is determined. In practice, the parameter set is overdetermined by measuring the impedance at typically 100 frequencies near the resonance, as shown in figure 2. Analogously, recording and fitting impedance data near each overtone yields a unique set of parameters (C_1, L_1, R_1) used to represent that specific QCM when operating at that overtone. The solid lines in shown figure 2 are the result of these iterative fitting routines to the impedance data and illustrate that the equivalent circuit model is an excellent representation of the actual QCM response.

If a viscoelastic film is deposited on the electrodes of the previously clean QCM device, an additional interfacial impedance arises due to the mechanical coupling of the film to the moving electrode. The measured electrical impedance data from the coated QCM will not be adequately represented by the equivalent circuit of the clean device and requires the additional model equivalent circuit elements L_2 and R_2. These conceptually represent energy stored and dissipated within the film, respectively [4]. By keeping the C_1, L_1, R_1 parameters fixed and fitting multi-frequency data from the coated QCM, the electrical parameters L_2 and R_2 are overdetermined.

Using acoustic theory, the additional electrical impedance, $Z_e(\omega)$, exhibited by the coated QCM can be related to the mechanical impedance at the QCM interface by the relation:

$$\text{Equation (1)}: \quad Z_e(w) = R_2 + iwL_2 = \frac{Np}{4K^2 w_s C_0}\left(\frac{Z_{\text{Interface}}}{Z_{\text{Quartz}}}\right)$$

where ω is the angular frequency ($\omega = 2\pi \bullet \nu$), N is the harmonic number (N = 1,3,5...), K is the unitless electromechanical coupling constant for quartz (7.74 x 10^{-3}), ω_s is the angular series resonant frequency (~$2\pi \bullet$5 MHz), C_o is the static capacitance, and Z_{QUARTZ} is 8.839 x 10^5 g/cm^2 sec [6]. For a QCM in contact with a viscoelastic film, the mechanical impedance at the interface can be written explicitly as a function of the film complex shear modulus, $\mathbf{G_{film}}$, film density, ρ_{film}, and film thickness, $\mathbf{L}_{film}$:

$$\text{Equation (2):}\quad Z_e(\omega) = R_2 + i\omega L_2 = \frac{N\rho}{4K^2\omega_s C_o Z_{QUARTZ}} \sqrt{r_{film} G_{film}} \tanh\left[i\omega L_{film} \sqrt{\frac{r_{film}}{G_{film}}} \right]$$

This is the essential equation that relates the film's mechanical properties to the experimentally observable electrical impedance. Note that if the film density and thickness are known -- both of which are assumed to be uniform -- then L_2 and R_2 will uniquely determine the complex modulus, $\mathbf{G}_{film} = G' + i \bullet G''$. Stated simply, this equation relates energy storage and dissipation within the film (expressed in electrical units) to the film modulus (mechanical units).

3.0 Results and Discussion

While great progress has been made in understanding structure and dynamics at the atomic level, applying this detailed understanding to mesoscale systems remains challenging. Phenomena such as wetting and spreading typically involve more than a few billion particles and occur over time scales many orders of magnitude greater than that of individual atomic motions. The key to tackling this problem is to identify the essential atomistic processes that control the energetics, and therefore the kinetics, of the overall ensemble process. For wetting and spreading, we focus upon the leading edge of the droplet where a small subset of particles (atoms or molecules) must advance from within the droplet to cover the previously exposed substrate surface. Evidence for a microscopically thin precursor layer, or "foot," preceding the macroscopic contact line between the droplet and substrate suggests that the process of wetting is controlled by the interactions of only a few liquid layers with the substrate. This implies that the viscoelastic properties of such ultra-thin layers are key to understanding spreading in general.

3.1 Self-Assembled Monolayers

We have shown above how the AWD technique may be used to determine the shear modulus of a thin film mechanically coupled to the electrodes of a quartz crystal microbalance. Our first objective was to show that the AWD technique has sufficient sensitivity to measure the viscoelastic properties of nanometer thick films. Whereas demonstrating sensitivity at this level is a noteworthy technical achievement, it is scientifically useful only if the measured ensemble film response can be related to the underlying molecular-scale structure and bonding. Therefore we selected two model systems consisting of simple organo-thiol molecules that self-assemble from solution onto the gold QCM electrodes. The resulting layer is a single monolayer of inclined molecules arranged in a two-dimensionally periodic c(4x2) array [7]. These self-assembled monolayers (SAMs) are not only good model systems for studying the relationship between atomic-scale structure and interfacial

viscoelastic properties, but also have practical application as effective lubricant layers in micro-machine sensor and actuator device [8,9].

The first SAM system is diacetylene thiol (DAT) molecules, $HS(CH_2)_{10}C\eth CC\eth C(CH_2)_{10}R$, where R is either COOH or CH_3. These experiments enabled us to test the sensitivity of AWD to viscoelastic changes when the *inter*molecular bonding is changed within the film. The second model system is the simpler *n*-alkane thiol monolayers, $HS(CH_2)_nCH_3$, where n = 11, 13, or 17. The purpose of these experiments is to probe the more subtle effect of molecular structure and ordering on the ensemble mechanical response.

The general experimental procedure for self-assembled monolayer experiments was similar for both model systems [9,10]. Commercially available QCM substrates with nominal series resonance at 5 MHz were used for all measurements. For some experiments, clean gold electrodes were prepared by pirhana etching the QCM, followed by rinsing in deionized water and ethanol. For other experiments, the pre-patterned electrodes were chemically removed from the quartz substrate, which was then solvent rinsed and ozone cleaned to remove any residual organic surface impurities. New electrodes were patterned onto the bare quartz substrates by vacuum deposition of a 150Å chromium binder layer followed by a 2000Å gold electrode layer. Three QCM substrates were patterned simultaneously along with two test coupons used for complementary diagnostics described below.

The clean QCM was mounted in a high vacuum chamber that was evacuated to better than $5x10^{-7}$ torr for the reference AWD measurements. The QCM substrate was then removed from the vacuum chamber and immediately immersed in a micromolar solution of the appropriate molecule for 12-24 hours to form the self-assembled monolayer. Following solution deposition, the coated QCM was thoroughly rinsed in pure solvent and remounted in the vacuum test chamber for the AWD film measurement. By making the measurements under vacuum, we reduce the probability of impurity adsorption onto the SAM and also simplify the data analysis, since there is no ambient atmosphere to which the QCM can acoustically couple.

Because temperature variations cause AWD effects comparable to the signal from nanometer scale films, a thermostatically-controlled cooling system was used to reproducibly maintain the QCM within 0.1_C of the desired temperature during both reference and coated QCM experiments. Impedance data were obtained with a Hewlett-Packard network analyzer at frequencies near the series resonance and the first four overtone frequencies. Details of the data acquisition and reduction methods are reported elsewhere [10,11].

Additional substrate and film quality characterizations were performed throughout these experiments. Atomic force microscopy was used to measure the rms roughness of the commercially deposited gold electrodes and the evaporated gold/chromium layer on our own test coupons. Whereas the commercial devices exhibited roughness values that ranged from 17Å to 35Å, much smoother surfaces (~4-8Å rms) were reproducibly obtained from our own deposition process.

Prior work by others with the SAM systems used herein provides the basic structural information needed to use equation 2 to interpret our AWD data, specifically, the film areal

density and thickness. However, spectroscopic ellipsometry (SE) proved to be a valuable check to ensure the complete coverage of the active electrode surface and to verify the actual film thickness. Because the unsaturated DAT films are susceptible to radiation damage, SE measurements on these films were always performed after the AWD experiment.

3.1.1 Diacetylene Thiol Experiments

Previous work by others [12] has shown that diacetylene thiol molecules, $HS(CH_2)_{10}C\eth CC\eth C(CH_2)_{10}R$, form c(4x2) overlayers on Au(111) as illustrated schematically in figure 4. More importantly for this study, the adsorbed layer can be photo-polymerized using UV light, resulting in a highly cross-linked film with increased stability in chemical sensor applications. Analogous to cross-linking of polymeric networks, we expect that the cross-linked DAT film should be stiffer than the virgin film, i.e., have a higher shear modulus. In the present studies, films terminating with either R=COOH or $R=CH_3$ were used. Whereas the carboxylic acid terminated molecules are more easily synthesized, the methyl terminated film is chemically inert to impurity adsorption from the ambient. Hence, comparison studies of the differently terminated films ensure that the observed effects are intrinsic to the internal film structure and not due to surface properties.

A second desirable feature of these DAT monolayers is that a second DAT molecule can be chemically linked to the -COOH group of the anchor molecule in the monolayer to form a longer chain, double diacetylene molecule [12]. This process can be repeated to build so-called "multi-layer" films that preserve the underlying order and therefore the two-dimensional packing of the monolayer. Note that while these thicker DAT films are denoted as "bilayers" and "trilayers" to indicate the number of molecules linked together, they are more properly a single layer of longer molecules, each of which is anchored to the gold substrate by its thiol head group.

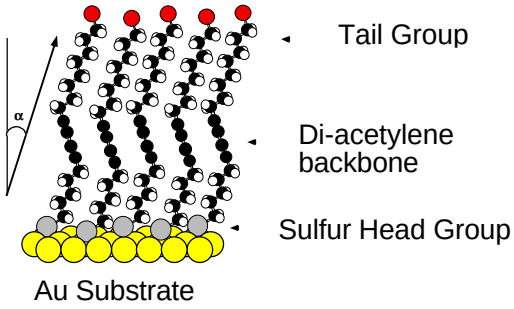

Fig. 4. Schematic representation of a self-assembled monolayer of DAT molecules on Au(111).

Monolayer and multi-layer DAT samples were routinely checked by Spectroscopic Ellipsometry (SE) after the AWD experiment to ensure film integrity. Briefly, SE measures the change in polarization of a monochromatic beam of light after reflection from a surface [13]. The complex refractive index of the substrate and film thereon determines the reflectivity of the s-polarized and p-polarized components. SE does not measure the reflectivity directly but instead measures tan ψ, where ψ equals the p to s magnitude ratio, and Æ, the phase difference between the two waves. Using known optical constants for the substrate and film, the film thickness is determined by iteratively modeling the SE data until satisfactory agreement is obtained. Figure 5 shows a representative result for a 3-layer DAT sample after photo-polymerization. These data, obtained at two angles of incidence, are well fit by a model consisting of a 68±1Å thick organic film on a clean gold substrate. This is consistent with an expected film thickness of ~72Å (using the 24Å thickness for the DAT monolayer).

After mounting the DAT-coated QCM in the test chamber, AWD data were obtained for the initial sample and after intervals of UV exposure. Because the UV source was in close proximity to the QCM device, sample heating occurred concurrently with UV irradiation. Data were taken only after the sample temperature had returned to the initial value to within 0.1C. Impedance data at the fundamental and three overtones were curve fit to extract the energy storage and dissipation following stepwise UV irradiation.

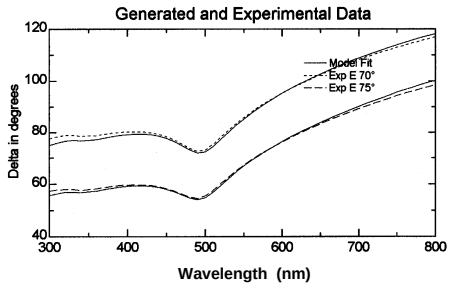

Fig. 5. Spectroscopic ellipsometry data and model fit for a tri-layer DAT film on a QCM substrate.

The AWD technique has enabled us to make the first ever measurement of the complex modulus for a single monolayer of adsorbed molecules [10,14]. We find a frequency-dependent storage modulus of 0.4 - 1.2 MPa for shear rates estimated to be ~0.05-1.0 m/sec, respectively. Changes for the DAT monolayer due to UV cross-linking were found to be extremely small and comparable to thermal effects alone, as shown by annealing experiments described elsewhere [10]. However, the multi-layer DAT films exhibited clear changes in the energy storage as shown in figure 6.

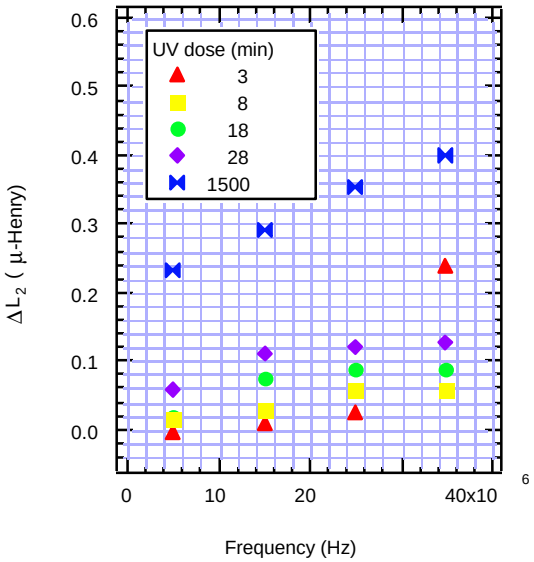

Fig. 6. Equivalent circuit analysis results for the energy storage in a 3-layer DAT film at the series resonant frequency and at higher harmonics, as a function of UV exposure.

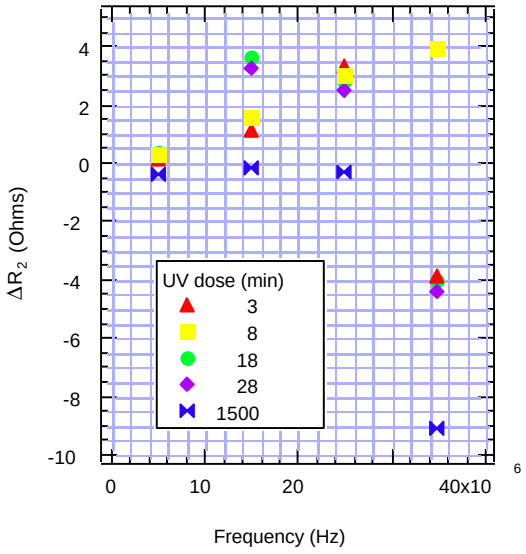

Fig. 7. Equivalent circuit data for the energy dissipation in a 3-layer DAT film at the series resonant frequency and at higher harmonics, as a function of UV exposure.

With the known film thickness and areal density, equation 2 can be used to calculate the shear modulus for the DAT film before and after photo-polymerization. One difficulty with this approach is that the DAT film deposition process does subtly alter the gold electrode surface, removing mass equivalent to 0.1 monolayer of gold atoms. This introduces a systematic error in the data analysis which slightly complicates the analysis of virgin and

polymerized DAT films. Alternately, the polymerized DAT film can be referenced to the virgin DAT film, thereby extracting a differential change in the shear modulus. While this approach eliminates the problem of an imperfect "clean" reference, it requires mathematical approximations to equations 1 and 2 in order to reduce the complex algebra to manageable forms. After analyzing our data using both approaches, we found that although the exact values for the elastic modulus differed, photo-polymerization consistently increased the elastic modulus by at least two orders of magnitude. Virgin DAT films have a modulus in the range of 10^6-10^7 dynes/cm^2 whereas the cross-linked values fall in the range from 10^8-10^9 dynes/cm^2 [10].

We note that in control experiments, annealing a DAT film without UV photo-polymerization does increase the storage modulus but not by more than a factor of five. A possible cause for this modulus increase with annealing is the thermal desorption of trace solvent molecules from within the film into the vacuum, thereby improving the molecular packing and ordering. Thus we conclude that the predominant cause of stiffening of the DAT film after UV irradiation is the intermolecular bonding that is absent in the virgin DAT film.

Figure 7 shows the energy dissipation data for the same cross-linking experiment. Unlike the energy storage data of figure 6, no systematic trend with increasing UV exposure is apparent. At the fundamental frequency, irradiation has a vanishingly small effect upon the dissipation within the film. However, at higher harmonics, some change is apparent at intermediate exposures but no net change occurs overall. Since ΔR_2 is most sensitive to the amplitude variations of the impedance response data, weaker signals at the higher harmonics and the choice of reference data lead to considerable error in the value of ΔR_2. Subsequent molecular dynamics simulations for the *n*-alkane thiols SAMs (discussed below) indicate that the atomistic origin of energy dissipation in these periodic overlayers is at defect sites. Hence, sample to sample variations among the DAT monolayers and "healing" of packing defects upon cross-linking would lead to both thermal and UV induced changes in the measured energy dissipation.

Finally, a comparison of cross-linking results for methyl terminated and carboxylic acid terminated DAT films showed comparable changes in both the ΔL_2 and the ΔR_2 values. For example, ΔL_2 = 0.047 μH and 0.058 μH and ΔR_2 = 1.0 Ohm and 0.4 Ohm. This is reasonable agreement considering that the domain structures of any two samples are unknown and may be considerably different. The similarity of results does support an interpretation based primarily upon bonding and structural changes within the films rather than the surface functionality.

3.1.2 *n*-Alkane Thiol Monolayer Experiments

The purpose of the *n*-alkane thiol SAM experiments is to develop a quantitative understanding of how differences in the constituent molecule structure and ensemble packing are manifested in the overall film viscoelasticity. The simplest systematic variation possible is the chain length of the *n*-alkane thiol molecule. This preserves the two-dimensional periodicity of the layer, shown in figure 8. Because van der Waals interactions control the alignment of the molecules, SAMs of shorter chain molecules are less well ordered [15] and therefore are expected to exhibit a different dynamic response to shear.

In order to properly investigate the subtle dynamic effects of varying chain length in these single monolayer experiments, sample integrity was essential. In addition to SE measurements to confirm the film thickness expected from prior work, we used Fourier Transform Infra-Red (FTIR) spectroscopy to check for impurities [16]. Additionally, FTIR is a sensitive probe of disorder within the SAM since disorder leads to inhomogeneous broadening of the vibrational bands. Reference FTIR spectra of the freshly evaporated gold QCM electrode surface and of the SAM were taken using p-polarized light incident at 80^0.

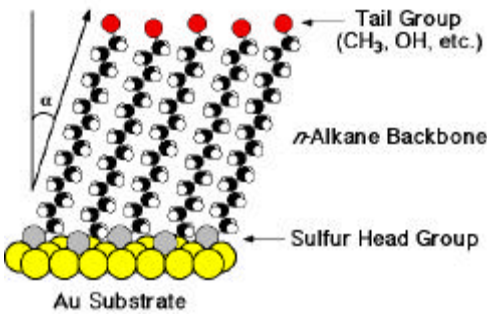

Fig. 8: Schematic representation of a self-assembled monolayer of linear *n*-alkane thiol molecules on a Au(111) substrate.

Figure 9 shows representative spectra for $C_{12}H_{26}S$ and $C_{18}H_{38}S$. All of the characteristic peaks of *n*-alkane thiol SAMs are present and appear in the correct region. Since the CH_2 stretching mode absorption intensity is directly related to the number of CH_2 units per alkyl group, the absorption peaks of $C_{18}H_{38}S$ at 2918 cm^{-1} and 2850 cm^{-1} are greater than those of $C_{12}H_{26}S$. The unbroadened FTIR spectra indicate that the SAMs are indeed well-ordered.

The results of the AWD measurements are summarized in figure 10 where the elastic shear modulus for SAMs of increasing chain length are plotted as a function of frequency. Each symbol represents the average of 5-10 samples. Two trends are obvious. Firstly, at the fundamental frequency (lower shear rates), the elastic shear modulus increases with chain length, from ~0.01 MPa (C_{12}) to ~0.1 MPa (C_{18}). Secondly, since our multi-frequency spectral analysis method allows us to obtain a modulus as a function of increasing shear rate, we find that short chain SAMs exhibit a significant modulus increase with shear rate [11].

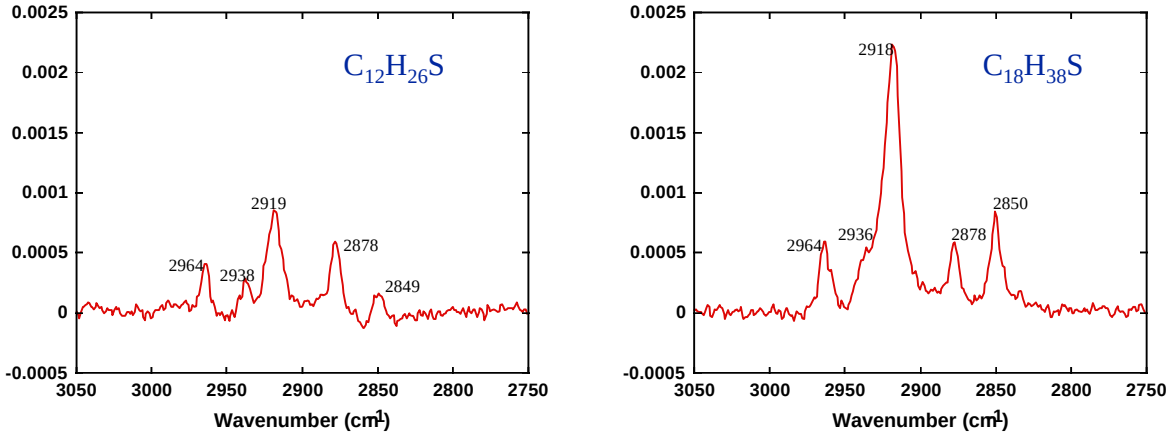

Fig. 9. Infra-red reflection spectra for $C_{12}H_{26}S$ and $C_{18}H_{38}S$ self-assembled monolayers on polycrystalline Au(111).

At present, we believe that both results originate from the loose molecular packing within short-chain monolayers. At low excitation frequencies, the loosely packed —and therefore sterically less restricted — short-chain molecules can respond in an incoherent fashion, somewhat similar to viscous polymeric solution behavior. If at higher frequencies, the conformational relaxation time is comparable to the period of oscillation, then a more solid-like response is observed. For longer chain SAMs, the increased van der Waals interactions that order the molecules leads to a coherent ensemble response even at the lower shear rates. Molecular dynamics simulations of short-chain SAM dynamics are planned to test this hypothesis.

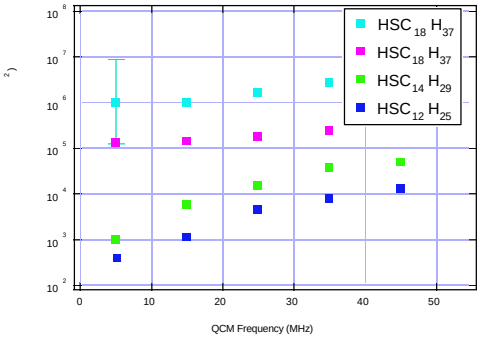

Fig. 10. Elastic shear modulus for *n*-alkane thiol SAMs as a function of frequency.

As with the diacetylene SAM films described above, the energy dissipation exhibited significant sample-to-sample variation and no correlation with hydrocarbon chain length. This is consistent with the hypothesis that the dominant source of energy dissipation is at the domain walls and not within the well-ordered domains. This could be tested by comparing SAMs grown on polycrystalline gold substrates with systematically larger average grain sizes.

3.1.3 Molecular Dynamics Simulations

Molecular dynamics simulations enable the atomic-scale viscoelastic properties measured by AWD to be related to atomic scale bonding and structure. For liquid metal and amorphous ceramic layers, these MD simulations provide the fundamental insights into flow and creep mechanisms. For our model molecular film studies, MD simulations provide a means by which we can understand how the elastic and dissipative components of the film modulus relate to the molecular bonding, order and interactions. We have performed simulations of a perfectly ordered monolayer of C_{16} *n*-alkane thiol molecules on Au(111) [11,17]. Using realistic potentials and periodic boundary conditions, the equilibrium geometry of the c(4x2) overlayer was first determined by energy minimization and found to be in excellent agreement with models based upon experimental results. By applying a static shear stress to the SAM, the force required to maintain a given deformation is obtained. After allowing for the molecular backbone to relax, a theoretical elastic modulus of >10 MPa is calculated. However, this is several orders of magnitude higher than the results obtained by AWD.

The key to understanding this discrepancy is recognizing that a static shear response differs from the dynamic shear of the AWD experiment. Inertially shearing the SAM by a high-frequency lateral translation of the gold substrate (analogous to the AWD experiment) reveals that the ensemble response involves azimuthal molecular rotation about the surface normal, rather than the expected one-dimensional molecular libration. This unexpected quasi-rotational motion is energetically preferable to one-dimensional shear and can account

for the lower measured storage modulus. At present, we are working on a reliable method to extract a dynamic storage modulus from the simulation in order to compare directly with the experimental value.

One advantage that our AWD experiment has over conventional approaches is that the characteristic time-scale is comparable to that of MD simulations. At our highest operating frequencies, the period of oscillation is approximately one nanosecond. Even with picosecond time-steps, an MD simulation can be run for this duration at reasonable cost. The rapid advances in code development for parallel processing (at Sandia and elsewhere) will make these nanosecond simulations routinely affordable.

Very recent simulations further show that the introduction of defects into the SAM leads to energy dissipation that is absent in the perfectly ordered monolayer [17]. We are exploring this issue in detail so that we may fully understand the results of our SAM experiments. This illustrates how realistic simulations and AWD experiments enable us to predict and verify the individual effects of molecular structure, intermolecular bonding, order, and impurity incorporation on the mechanics of real films.

3.2 Liquid Indium Experiments

The absolute sensitivity of the QCM to sub-monolayer mass changes is well known. It's sensitivity to viscoelastic properties and changes therein at the molecular monolayer level have been demonstrated above. The ability to detect a phase change (melting) and to measure the viscoelastic properties at the nanometer level at *elevated temperature* is a significant technical challenge. In order to explore the feasibility of AWD measurements, we built a simple high vacuum apparatus containing a QCM device, radiative heater, and evaporator for *in situ* deposition of low melting temperature metals.

We first used this system to measure the resonant frequency shift of commercial QCM substrates as they are temperature cycled to ~200_C in vacuum. Because the coefficient of thermal expansion of AT-cut quartz varies considerably with small changes in crystallographic orientation, most commercial QCM devices are oriented to minimize this thermal coefficient in a narrow temperature range around the expected operating temperature, typically 25_C. Once the temperature exceeds this narrow range (±5C), the coefficient of thermal expansion exhibits non-linear behavior and the resonant frequency becomes a strongly varying function of the device temperature [4]. Our tests with the commercial QCM devices confirm that the thermal effect upon the frequency shift is indeed large.

We then vapor deposited indium films of ~1-5 micron thickness onto a QCM in vacuum, and radiatively heated the device above the melting point of indium (156_C). These experiments were compared to control experiments without the indium films. Figure 11 shows a typical result for a ~1 micron thick indium film, initially vapor deposited at 25_C. As the temperature was increased through the melting temperature, a rapid 200 Hz frequency deviation occurred, which was superimposed upon the monotonic frequency increase due to thermal expansion of the resonator alone. Upon cooling to room temperature, a similar transient appeared superimposed upon the slowly decreasing frequency of the cooling and

contracting resonator. The lower panel shows the rapid onset of ~2 volts DC of acoustic damping signal upon melting, and its sudden quenching upon re-solidification. This extremely strong signal above the indium melting temperature is overwhelming evidence that the oscillator is in contact with liquid indium. Proportionately smaller damping voltages are obtained for thinner layers. In future measurements where the thickness and film morphology are known, the quantitative damping voltage can be converted to an effective viscosity of the micron to nanometer thick liquid metal layer.

We are now working to improve the temperature accuracy and eliminate the temperature gradient across the sensor surface so that we can study possible pre-melting phenomena. In order to interpret the AWD response for increasingly thinner liquid metal layers, we must know the interfacial composition and structure on the atomic scale. Ultra-high vacuum conditions and surface analytical techniques are required to establish the cleanliness, morphology and chemical composition of the interfacial liquid metals.

Although these preliminary results are encouraging, the application of AWD to atomic-scale fluid flow at solid interfaces requires continued technology development in both the sensor design and its associated electronics. In the previous work, we used commercially available QCM sensors to evaluate their sensitivity and suitability for liquid metal experiments. While these are acceptable for thin film studies and could possibly be used for elevated temperature experiments, they are far from ideal. Specifically, the exact crystallographic orientation of the single crystal quartz wafer used in commercial QCM sensors is deliberately chosen to minimize the temperature dependence of the resonant frequency at 25_C. Hence, for typical applications near 25_C, the QCM is relatively insensitive to minor temperature fluctuations. However, away from this optimal temperature, the resonant frequency exhibits an exponentially increasing temperature dependence that makes the sensor unstable for viscoelastic measurements.

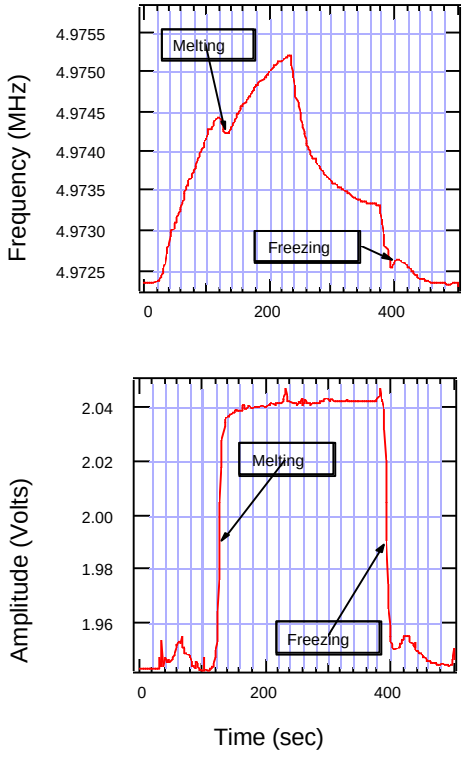

Fig. 11: AWD response to heating and cooling a micron thick indium film on a tantalum substrate: (upper panel) Frequency changes as the device temperature is first raised and then lowered through the indium melting temperature; (lower panel) Acoustic wave amplitude change due to acoustic wave propagation into the liquid indium layer. Increased voltage corresponds to energy dissipated within viscous indium layer.

The second limitation is that conventional oscillator circuits are designed to track the damping at only the series resonant frequency. However, as the sensor temperature is varied over several hundred degrees, resonant frequency shifts due to thermal expansion and discontinuities due to mode exchanges cannot be accurately tracked using these conventional oscillator circuits. As shown in figure 12, additional modes are excited and couple to the fundamental thickness shear mode. As the temperature is varied over just a few degrees, amplitude is exchanged between these modes.

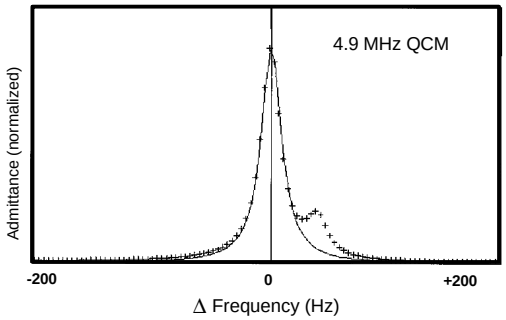

Fig. 12: Admittance plot vs. frequency showing the onset of vibrational mode coupling near the fundamental resonance.

Circuits that track only the frequency at the peak admittance will erroneously "jump" between modes and yield false amplitude data under these conditions. However, by recording the full impedance spectrum, we can readily distinguish these temperature-dependent effects in the sensor from viscoelastic changes in the material under study. This capability is critical for studies of melting, flow, and liquid/solid interfacial reactions.

Therefore, we have begun the design and fabrication of prototype sensors specifically for elevated temperature experiments. The QCM configuration remains our chosen sensor due to the simplicity of interpreting and modeling the pure transverse shear modes of the resonator. Our strategy is to use a differential signal approach to nullifying the intrinsic thermal response of the QCM. Specifically, we have patterned two QCM resonators on one quartz crystal, as shown in figure 13, each with a slightly different electrode thickness to shift their resonant frequencies by 10-100 Hz. This is done to minimize acoustic interference effects. By operating one QCM as a reference experiment while conducting an AWD experiment on the other QCM, we can use the differential signal to extract the relevant phase change and damping signals [18]. Preliminary results are encouraging but additional design work is needed to prevent cross-talk between the resonators.

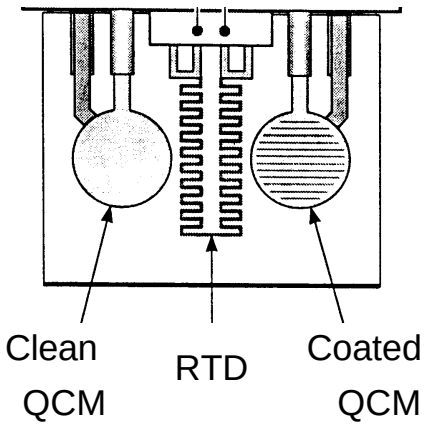

Fig. 13: Schematic of custom fabricated dual QCM sensor device with patterned resistive temperature device.

Using our prototype high-temperature QCM sensor, we have made the first viscoelastic measurements of melting and solidification in nanometer-scale liquid metal layers [19]. A solid indium film is vapor deposited onto tantalum or chromium electrodes of a quartz

crystal microbalance sensor in ultra-high chamber. Gold electrodes are not used since alloying with indium would complicate interpretation of the AWD response. The frequency shift of the sensor during indium deposition provides an accurate measure of the solid layer thickness. The sensor is then slowly heated while continuously recording the damping response. Melting of the indium layer is indicated by a dramatic damping of the resonator amplitude as well as a frequency shift downward.

These two results are unambiguous indicators of melting of the indium layer. Upon slow cooling of the 10-50 nm thick indium layers, resolidification does not occur until as much as 30_ below the bulk melting temperature. This undercooling is found to be reproducible for a given indium layer.

Liquid metal undercooling is known to occur in microscopic phase-separated domains of intermetallic alloys. The resultant microstructure can have important consequences for material performance. We intend to further explore the undercooling phenomenon in nanoscale liquid metal layers. With the addition of surface analysis techniques to provide information about the liquid layer morphology and composition, we will be able to directly study the viscoelastic properties of undercooled interfacial liquid metal layers.

4.0 Conclusions

Acoustic Wave Damping has been used for viscoelastic measurements of nanometer scale molecular layers and liquid metals. This accomplishment required new technology development, including QCM sensor mounting, detection electronics and fabrication of a differential sensor compatible with ultra-high vacuum surface analysis techniques.

Using self-assembled monolayers, we have shown that the AWD technique indeed has the required sensitivity to quantitatively measure viscoelastic properties of ultra-thin films. We used photo-polymerization to demonstrate sensitivity to intermolecular bonding within a film, and *n*-alkane thiol SAMs to show the effect of film structure on mechanical properties. Molecular dynamics simulations were instrumental in relating the ensemble response measured by AWD to the motions of the constituent molecules. The results to date suggest that the choice of constituent molecule can be used to engineer the elastic shear modulus of a monolayer film, whereas its loss modulus is controlled by the defect density within the film. From such studies, we can gain a molecular level understanding of thin film viscoelastic behavior that controls lubrication, adhesion, and vibration damping in micromotors and sub-micron devices.

Elevated temperature AWD experiments present significant challenges due primarily to temperature effects in the QCM sensor that are larger in magnitude than the damping signal from the liquid layer. However, by using a spectrum analysis approach and a prototype differential AWD sensor, we were able to show that nanometer scale metal melting experiments are feasible. Our present results clearly demonstrate the ability of our new experimental approach to quantify the unique thermal/physical properties of thin interfacial wetting layers and point to significant differences in thin layer properties between the micron and nanometer thickness scales that can dramatically impact the formation and stability of joined interfaces.

Acknowledgment

This work was performed under the Laboratory Directed Research and Development program at Sandia National Laboratories. Sandia is a multiprogram laboratory operated by Sandia Corporation, a Lockheed Martin Company, for the United States Department of Energy under Contract DE-AC04-94AL85000. The authors gratefully acknowledge the valuable contributions of Stephen J. Martin, Thomas Schneider, Richard Cernosek, Mary-Anne Mitchell, Ross Thomas, James Spates, and Antonio J. Ricco to this work.

References

1. A. Mortensen, V. J. Michaud and M. C. Flemings, J. Metals, Jan. 1993, p.36; D. W. Keefer, S. A. David, H. B. Smart and K. Spence, J. Metals, Sept. 1993, p.6.

2. P.G. deGennes, Rev. Mod. Phys. **57**, 827 (1985); T. D. Blake, "Dynamic Contact Angles and Wetting Kinetics, " in *Wettability* ed. by J. C. Berg, (Marcel Dekker, NY, 1990); S. F. Kistler, "Hydrodynamics of Wetting," *Ibid.*

3. T. Young, Philos. Trans. R. Soc. London **95**, 65 (1805).

4. *Applications of Piezoelectric Quartz Crystal Microbalances*., C. Lu and A. W. Czanderna, eds., (Elsevier, New York, 1984).

5. C. D. Stockbridge, in*Vacuum Microbalance Techniques*, K. H. Behrndt, ed. (Plenum, NY, 1966) Vol. 5, p. 193.

6. S. J. Martin, V. E. Granstaff and G. C. Frye, Anal. Chem **63**, 2272 (1991); S. J. Martin and G. C. Frye, IEEE, 1991 Ultrasonics Symposium, page 393.

7. G. E. Poirier, M. J. Tarlov and H. E. Rushmeir, Langmuir **10**, 3383 (1994).

8. A. Ulman, *An Introduction to Ultrathin Organic Films From Langmuir-Blodgett to Self-Assembly* (Academic Press, San Diego, 1991).

9. M. D. Porter and M. M. Malczak, *Handbook of Surface Imaging Visualization*. (CRC Press, Boca Raton, 1995) pp. 733-40.

10. N. D. Shinn, T. Kim, C. Daly, T. M. Mayer, R. M. Crooks, and T. A. Michalske, Langmuir (in preparation).

11. N. D. Shinn, T. A. Michalske, R. Limary, C. Daly, and U. Landman, Langmuir (in preparation).

12. T. Kim, R. M. Crooks, M. Tsen and L. Sun, J. Am. Chem. Soc. **117**, 3963 (1995).

13. R. M. A. Azzam and N. M. Bashara, *Ellipsometry and Polarized Light* (North Holland, Amsterdam, 1977).

14. A. J. Ricco, A. W. Staton, R. M. Crooks and T. Kim, Faraday Discussions (submitted).

15. M. D. Porter, T. B. Bright, D. L. Allara and C. E. D. Chidsey, J. Am. Chem. Soc. **109**, 3559 (1987).

16. R. Limary, "Dependence of Chain Length in Shear Modulus of *n*-Alkane Thiol Self-Assembled Monolayers," OSSP Final Report (unpublished).

17. U. Landman, private communication.

18. See: S. J. Martin, R. W. Cernosek and J. J. Spates, Transducers 95: Procedings, 8th Int. Conf. on Solid State Sensors, p. 712; S. J. Martin, G. C. Frye and K. O. Wessendorf, Sensors and Actuators A44, 209 (1994).

19. N. D. Shinn and C. Daly, (unpublished).

Appendix

List of publications resulting from this project:

"Nanomechanics of Self-Assembled Diacetylene Films," N. D. Shinn, T. A. Michalske, S. J. Martin, A. J. Ricco, C.L. Daly, J. Krim, T. Kim, H. Yang and R. M. Crooks, Bull. Amer. Phys. Soc., 1996 SAND95-2965A

"Nanomechanical Measurements of Diacetylene-Thiol Self-Assembled Monolayers by Acoustic Wave Techniques," N. D. Shinn, T. Kim, C. Daly, T. M. Mayer, R. M. Crooks, and T. A. Michalske, Langmuir (in preparation).

"Viscoelastic Response of Self-Assembled *n*-Alkane Thiol Monolayers to Shear," N. D. Shinn, T. A. Michalske, R. Limary, C. Daly, and U. Landman, Langmuir (in preparation).

"Acoustic Wave Damping Measurements of Undercooling in Nanometer-Scale Indium Layers," N. D. Shinn and C. Daly, Physical Review B (in preparation).

List of Presentations resulting from this project:

"Viscoelastic Properties of Langmuir-Blodgett Films Measured by Acoustic Wave Damping," N. D. Shinn, J. A. Mann and S. A. Martin, Fall Meeting of the Materials Reseach Society, Boston, MA, November 1994. SAND94-1697A

"Viscoelastic Properties of Molecular Films Measured by Acoustic Wave Damping," N. D. Shinn, T. W. Schneider, A. J. Ricco, S. J. Martin, T. A. Michalske,J. A. Mann, T. Kim, H. Yang and R. M. Crooks, Annual Meeting of the American Physical Society, San Jose, CA, March 1995. SAND94-2990A

"Viscoelastic Properties of Ultra-Thin Liquid Metals Measured by Acoustic Wave Damping," N. D. Shinn, T. A. Michalske and S. J. Martin, 9th International Conference on Liquid and Amorphous Metals, Chicago, IL, August 1995. SAND95-0442A

"Viscoelastic Properties of Molecular Films Measured by Acoustic Wave Damping," N. D. Shinn, T. W. Schneider, A. J. Ricco, S. J. Martin, T. A. Michalske, J. A. Mann, T. Kim, H. Yang and R. M. Crooks, National Symposium of the American Vacuum Society, Minneapolis, MN, October 1995. SAND95-1054A

"Viscoelastic Properties of Self-Assembled Diacetylene Films," N. D. Shinn, A. J. Ricco, S. J. Martin, T. A. Michalske, T. Kim, H. Yang, R. M. Crooks, C. L. Daly and J. Krim, Spring Meeting of the Materials Reseach Society, San Francisco,CA, April 1996. SAND95-2670A

"Nanomechanics of Self-Assembled Diacetylene Films," N. D. Shinn, T. A. Michalske, S. J. Martin, A. J. Ricco, C.L. Daly, J. Krim, T. Kim, H. Yang and R. M. Crooks, Annual Meeting of the American Physical Society, St. Louis, MO, March 1996. SAND95-2965A

"Mechanics of Self-Assembled Monolayers: Measurement and Atomistic Simulations," N. D. Shinn, T. W. Schneider, T. A. Michalske, U. Landman, T. Kim, and R. M. Crooks, National Symposium of the American Vacuum Society, Philadelphia, PA, October 1996. SAND96-1214A

"Dynamics of Alkane-Thiol Monolayers: Experiment and Atomistic Simulations," N. D. Shinn, T. W. Schneider, S. J. Martin, T. A. Michalske and U. Landman, Fall Meeting of the Materials Reseach Society, Boston, MA, December 1996. SAND96-1709A

"Molecular Monolayer Dynamics: Atomistic Potentials and Ensemble Responses," N. D. Shinn, T. A. Michalske, C. Daly, U. Landman, National Symposium of the American Vacuum Society, San Jose, CA, October 1997. SAND97-1253A

List of invention disclosures: None

List of patents: None

List of copyrights: None

Information regarding employee recruitment: Not applicable

Information regarding involvement of post-docs: This project partially supported a post-doctoral staff member, Christopher Daly, from September through December 1996. Dr. Daly explored various methods to conduct AWD measurements at elevated temperatures for the liquid metal experiments.

Information regarding involvement of students: One graduate student, Christopher Daly (Physics, Northeastern University), was hired under the Outstanding Summer Student Program from July through October 1995. Mr. Daly participated in the initial AWD experiments of molecular LB and SAM films. One undergraduate student, Ms. Ratchana Limary (Chemical Engineering, University of New Mexico), was supported from June-August 1996. Ms. Limary conducted AWD experiments of *n*-alkane thiol monolayers.

DISTRIBUTION:

3	MS0780	N. D. Shinn, 1114
1	MS1413	T. M. Mayer, 1114
1	MS1413	T. A. Michalske, 1114
1	MS1436	LDRD Office, 4523
1	MS9018	Central Technical Files, 8940-2
5	MS0899	Technical Library, 4916
2	MS0619	Review & Approval Desk, 12690 for DOE/OSTI